Particle Accelerators, 1992, Vol. 39, pp.137–146
Reprints available directly from the publisher
Photocopying permitted by license only

INVERSE COMPTON SCATTERING OF THERMAL RADIATION AT LEP AND LEP-200

ANTONIO DI DOMENICO

Dipartimento di Fisica, Università "La Sapienza", I-00185 Rome, Italy
and INFN Sezione di Roma, Rome, Italy

(Received 2 March 1992; in final form 10 June 1992)

In this paper the kinematics of inverse Compton scattering is reviewed and applied to thermal radiation scattered by an electron (or positron) beam. Evaluations of energy spectrum and rate of scattered photons are made in the case of LEP and LEP-200. Furthermore influence of this process on the stored beam lifetime is estimated.

KEY WORDS: Inverse Compton Scattering, LEP, LEP-200

1 INTRODUCTION

In a particle accelerator, from a general point of view, the vacuum pipe in which the beam circulates can be considered a black body cavity at room temperature. Hence an electromagnetic radiation in thermal equilibrium is present inside the pipe with an energy distribution following the Planck's law. Such radiation may be scattered by the beam travelling inside the pipe (inverse Compton scattering) and it can gain, after the scattering, a significant amount of the beam energy†. For example a thermal photon of energy $k = 0.07$ eV (the mean energy of thermal photons at room temperature) can emerge with an energy $k' \simeq 2.8$ GeV after an inverse Compton back-scattering experienced in a head-on collision with a 50 GeV electron.

The Large Electron Positron collider (LEP) at CERN is the first accelerator in which the high energy photons produced in the inverse Compton scattering of thermal radiation have been observed[1,2]. In fact the exceptionally low residual gas pressure obtained in the LEP vacuum pipe ($\sim 2.2 \times 10^{-10}$ torr) has made this measurement possible reducing the background due to the beam-gas bremsstrahlung.

In the following the expected energy spectrum and rate of scattered thermal photons at LEP and LEP-200 will be evaluated and in the case of LEP it will be compared to data

† Also pair production may occur in the interaction of the beam with thermal photons, but only if the photon energy in the beam particle rest frame exceeds the threshold for this process. In actual or designed accelerators this condition is not satisfied at room temperature. Therefore we will restrict our considerations only to inverse Compton scattering.

taken by the LEP-5 experiment[1]. Furthermore the beam lifetime related to this process will be estimated.

As this work has been conceived within the framework of the LEP-5 experiment, whose main aim is a fast luminosity measurement at LEP by detecting the beam-beam single bremsstrahlung photons, some of the results that will be given have already been used in the analysis of the LEP-5 data.

Inverse Compton scattering occurring in the passage of a high-energy electron beam through a photon gas has been treated in the past by some authors mainly with a view toward astrophysical applications[3,4,5,6,7]. Since some of these calculations were approximated or affected by misunderstandings, we prefer to base our evaluations on exact formulas derived here and to perform the needed integrations by means of Monte Carlo methods.

2 DEFINITIONS

In this paper we adopt the usual units with $\hbar = c = 1$. The following definitions are given for the symbols of kinematic quantities and constants used:

E , $\vec{\mathbf{p}}$ are the primary electron energy and momentum, respectively, in the laboratory system;

k , $\vec{\mathbf{k}}$ are the primary photon energy and momentum, respectively, in the laboratory system;

k' , $\vec{\mathbf{k}}'$ are the scattered photon energy and momentum, respectively, in the laboratory system;

k^* , $\vec{\mathbf{k}}^*$ are the primary photon energy and momentum, respectively, in the electron rest frame;

$k^{*\prime}$, $\vec{\mathbf{k}}^{*\prime}$ are the scattered photon energy and momentum, respectively, in the electron rest frame;

$k_{\|}^*$, $k_{\perp}^*$ are the parallel and perpendicular components, respectively, of the photon momentum $\vec{\mathbf{k}}^*$ with respect to the Lorentz transformation direction (see Sect.3);

$k_{\|}^{*\prime}$, $k_{\perp}^{*\prime}$ are the parallel and perpendicular components, respectively, of the photon momentum $\vec{\mathbf{k}}^{*\prime}$ with respect to the Lorentz transformation direction (see Sect.3);

ψ , ζ are the incidence angles of the primary photon momentum with respect to the Lorentz transformation direction in the laboratory and electron rest frame respectively (see Sect.3) ;

θ , ϕ are the polar and azimuthal angles, respectively, of the scattered photon momentum $\vec{\mathbf{k}}^{*\prime}$ with respect to the $\vec{\mathbf{k}}^*$ direction;

χ is the angle between the scattered photon momentum $\vec{\mathbf{k}}'$ and the electron momentum $\vec{\mathbf{p}}$;

r_0 is the classical electron radius;

m is the electron rest mass;

K_b is the Boltzmann constant.

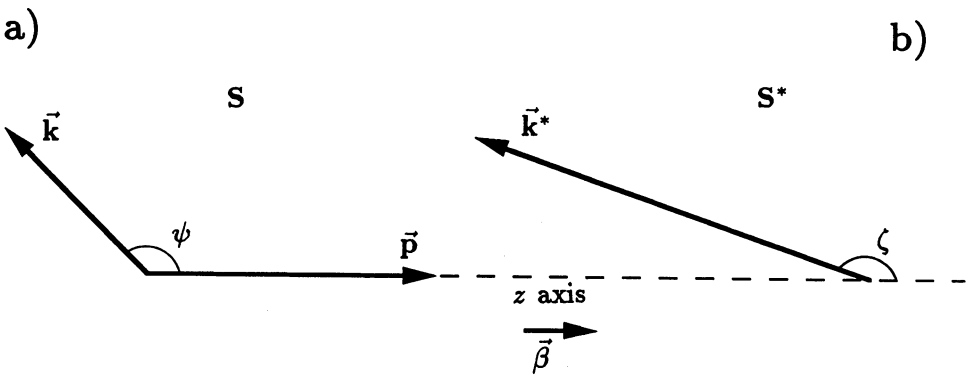

FIGURE 1: Graphic sketch for incident angles definitions in the laboratory system (a) and in the electron rest frame (b).

3 KINEMATICS

Let us consider a collision between a photon and an electron moving in the direction of the z axis in the laboratory system **S** (see Fig.1a).

The Lorentz transformation of the photon 4-momentum from **S** to the electron rest frame **S*** (see Fig.1b) is given by:

$$\begin{pmatrix} k^* \\ k^*_{\parallel} \end{pmatrix} = \begin{pmatrix} \gamma & -\gamma\beta \\ -\gamma\beta & \gamma \end{pmatrix} \begin{pmatrix} k \\ k\cos\psi \end{pmatrix} \quad , \quad k^*_{\perp} = k\sin\psi \tag{1}$$

where k and k^* are the primary photon energy in **S** and **S*** respectively; $k^*_{\parallel}$ and $k^*_{\perp}$ are the components of the primary photon momentum $\vec{\mathbf{k}}^*$ (in the **S*** frame) parallel and perpendicular to the z axis; ψ is the incidence angle between the photon and electron directions in **S** (see Fig.1a); β and γ are:

$$\beta = \frac{|\vec{\mathbf{p}}|}{E}$$

$$\gamma = \left(1-\beta^2\right)^{-1/2} = \frac{E}{m}$$

where E and $\vec{\mathbf{p}}$ are the primary electron energy and momentum respectively. From eq.(1) we get the incidence angle ζ in **S*** (see Fig.1b):

$$\tan\zeta = \frac{k^*_{\perp}}{k^*_{\parallel}} = \frac{\sin\psi}{\gamma(\cos\psi - \beta)} \tag{2}$$

Let us call θ and ϕ the polar and azimuthal angles of the scattered photon momentum $\vec{\mathbf{k}}^{*\prime}$ in **S*** respect to the $\vec{\mathbf{k}}^*$ direction. If we choose two orthogonal and unitary vectors $\hat{\mathbf{u}}$ and $\hat{\mathbf{v}}$ both perpendicular to the $\vec{\mathbf{k}}^*$ direction we have:

$$\vec{\mathbf{k}}^{*\prime} = k^{*\prime}\left[(\cos\theta)\hat{\mathbf{k}}^* + (\sin\theta\cos\phi)\hat{\mathbf{u}} + (\sin\theta\sin\phi)\hat{\mathbf{v}}\right]$$

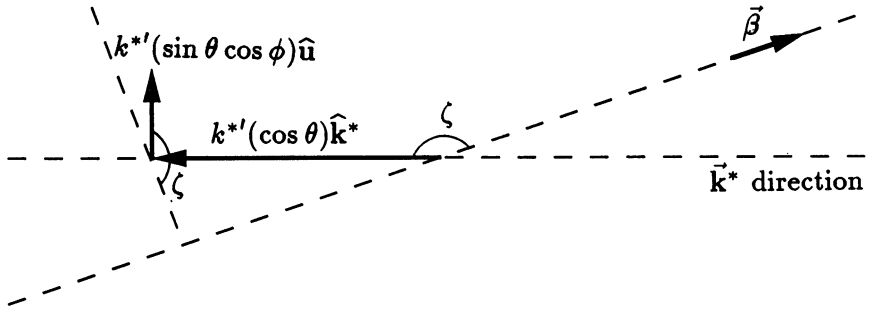

FIGURE 2: Decomposition of the scattered photon momentum $\vec{\mathbf{k}}^{*\prime}$ in the $(\vec{\beta}, \vec{\mathbf{k}}^*)$ plane.

If $\hat{\mathbf{u}}$ lies in the $(\vec{\beta}, \vec{\mathbf{k}}^*)$ plane ($\vec{\beta} = \vec{\mathbf{p}}/E$ corresponds to the Lorentz's boost direction) we obtain the situation sketched in Fig.2 . The component of $\vec{\mathbf{k}}^{*\prime}$ along $\vec{\beta}$ is :

$$k_{\|}^{*\prime} = k^{*\prime}(\cos\theta\cos\zeta + \sin\theta\sin\zeta\cos\phi) \tag{3}.$$

The Lorentz transformation of the scattered photon 4-momentum from **S*** to **S** gives:

$$k' = \gamma(k^{*\prime} + \beta k_{\|}^{*\prime}) \tag{4}$$

that combined with eq.(3) becomes

$$k' = k^{*\prime}\gamma\,[1 + \beta(\cos\theta\cos\zeta + \sin\theta\sin\zeta\cos\phi)] \tag{5}.$$

In the electron rest frame **S*** the energy of the scattered photon is given by the well known relation for the usual Compton scattering:

$$k^{*\prime} = \frac{k^*}{1 + \dfrac{k^*}{m}(1 - \cos\theta)} \tag{6}$$

From eq.(1) we get:

$$k^* = \gamma k(1 - \beta\cos\psi) \tag{7}$$

Finally substituting (6) and (7) in (5) we obtain:

$$k' = \frac{k(1 - \beta\cos\psi)\gamma^2\,[1 + \beta(\cos\theta\cos\zeta + \sin\theta\sin\zeta\cos\phi)]}{1 + \dfrac{k}{m}\gamma(1 - \beta\cos\psi)(1 - \cos\theta)} \tag{8}.$$

We would like to stress that the last relation can be considered a generalization of eq.(6) to moving electrons, it has been obtained without any approximation and it is necessary for a Monte Carlo evaluation of the scattered photon energy spectrum.

Now let us consider the angular distribution of the scattered photons in the laboratory system. It is easy to see that in the high energy limit ($\beta \to 1$) it is very close to the primary electron direction. In fact the transformation of the scattered photon 4-momentum from $\mathbf{S}^*$ to $\mathbf{S}$ gives:

$$k'_{\|} = \gamma k^{*\prime} [(\cos\theta \cos\zeta + \sin\theta \sin\zeta \cos\phi) + \beta] \tag{9}$$

and from eq.(4) and eq.(9) we get the cosine of the angle χ between $\vec{\mathbf{k}}'$ and $\vec{\mathbf{p}}$:

$$\cos\chi = \frac{k'_{\|}}{k'} = \frac{\alpha_{\|} + \beta}{1 + \alpha_{\|}\beta}$$

where we have defined $\alpha_{\|} = (\cos\theta \cos\zeta + \sin\theta \sin\zeta \cos\phi)$; so in the high energy limit $\cos\chi \to 1$.

4 RATE AND SPECTRUM OF SCATTERED THERMAL PHOTONS AND BEAM LIFETIME

In the case of thermal photons the differential density $dn = n(k, \vec{\mathbf{i}})dkd\Omega$, that denotes the number of photons per unit volume with energies within dk moving in the direction defined by the unit vector $\vec{\mathbf{i}}$ and the element of solid angle $d\Omega$, is given by the Planck distribution:

$$dn = n(k, \vec{\mathbf{i}})dkd\Omega = \frac{k^2}{\pi^2} \frac{dk}{(\exp[k/K_bT] - 1)} \frac{d\Omega}{4\pi}$$

where T is the beam pipe temperature and K_b the Boltzmann constant. Denoting as usual by * quantities measured in $\mathbf{S}^*$, the number of scattered thermal photons per unit time per electron is given by:

$$\frac{dN}{dt} = \frac{1}{\gamma}\frac{dN}{dt^*} = \frac{1}{\gamma}\int \sigma_c^*(k^*)dn^* \tag{10}$$

where $\sigma_c^*(k^*)$ is the Klein-Nishina total cross section[8]:

$$\sigma_c^*(k^*) = 2\pi r_0^2 \left[\left(\frac{1}{x} - \frac{4}{x^2} - \frac{8}{x^3}\right)\ln(1+x) + \frac{1 + x/2}{(1+x)^2} + \frac{8}{x^2}\right]$$

with

$$x = \frac{2k^*}{m}$$

In virtue of the relativistic invariance of the quantity[7] $\frac{dn}{k}$ and using the relation (7) we get :

$$dn^* = \gamma(1 - \beta\cos\psi)dn$$

and eq.(10) may also be written

$$\frac{dN}{dt} = \int \sigma_c^*(k^*)(1 - \beta\cos\psi)dn \tag{11}$$

The behaviour of $\frac{dN}{dt}$ as a function of the electron energy E at a temperature $T = 291°K$ is shown in Fig.3. It can be noted that $\frac{dN}{dt}$ reaches a plateau at low electron energies that corresponds to the Thomson limit for the cross section $\sigma_c^*(k^*)$. Fig.4 shows $\frac{dN}{dt}$ versus T at a fixed electron energy $E = 45.6$ GeV.

The energy spectrum of scattered thermal photons may be obtained from eq.(11) substituting in the integral the total Compton cross section $\sigma_c^*(k^*)$ with the differential one[6] in dk'. Another way to evaluate the spectrum is by means of a Monte Carlo integration of eq.(8), taking the spectrum normalization from the total rate in eq.(11). The latter is the method we have adopted. Results will be given in the next Section.

An interesting aspect concerning the scattering of thermal photons is its influence on the stored beam lifetime. Assuming that an electron leaves the beam if in the scattering it loses an energy greater than ΔE, the beam lifetime[‡] τ_{tp} related to thermal photon scattering is given by:

$$\tau_{tp} = \left(f(\Delta E) \frac{dN}{dt} \right)^{-1} \tag{12}$$

where $f(\Delta E)$ is the fraction of recoil electrons that have lost an energy greater than ΔE.

5 EVALUATIONS IN THE CASE OF LEP AND LEP-200

The number of scattered thermal photons per electron per unit of path travelled by an electron is

$$\frac{dN}{dz} = \frac{1}{\beta} \frac{dN}{dt} \tag{13}$$

The total rate of scattered thermal photons over the entire LEP straight section (~ 600 mt) may be deduced from eq.(13). For 1 mA total electron current (there are $N_e \simeq 1.37 \times 10^{11}$ electrons per bunch) and a pipe temperature $T = 291°K$ the rate N per bunch passing in the straight section in the case of a 45.6 GeV electron beam (LEP) is:

$$N = 2.65 \text{ per bunch passing}$$

while in the case of a 100 GeV electron beam (LEP-200) we get:

$$N = 2.56 \text{ per bunch passing}$$

The total rate is practically the same in both cases. In Fig.5 the energy spectra of scattered photons that correspond to these two cases are evaluated as explained in the preceding Section. Spectra obtained as for the previous ones but for different temperatures and only in the case of LEP are shown in Fig.6. We can observe that approximately the spectrum *end point* scales quadratically with the beam energy and linearly with the pipe temperature.

In Fig.7 it is shown the distribution of the total energy E_T of the photons produced in the LEP straight section 1, measured at each bunch passing with the LEP-5 electromagnetic

‡ Here the beam lifetime is defined as the time needed to reduce the beam intensity by a factor 1/e.

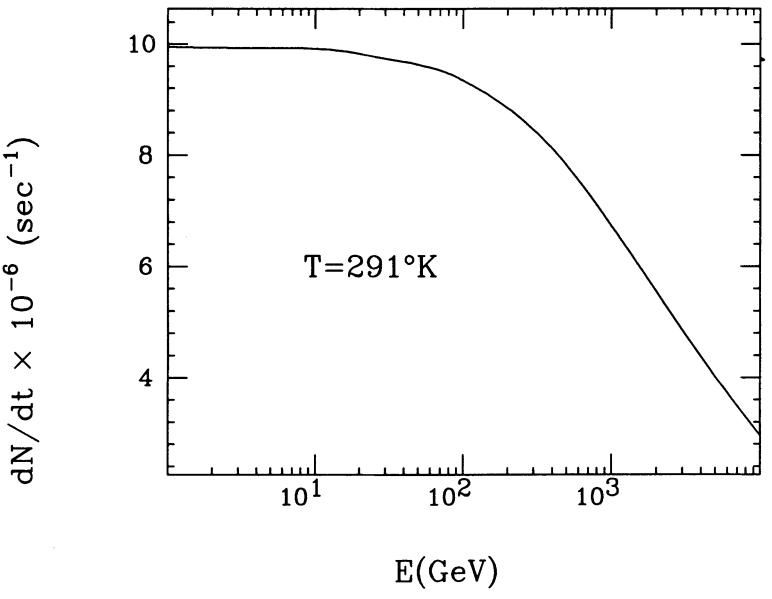

FIGURE 3: The rate $\frac{dN}{dt}$ of scattered thermal photons vs the electron beam energy E at a fixed pipe temperature $T = 291°K$.

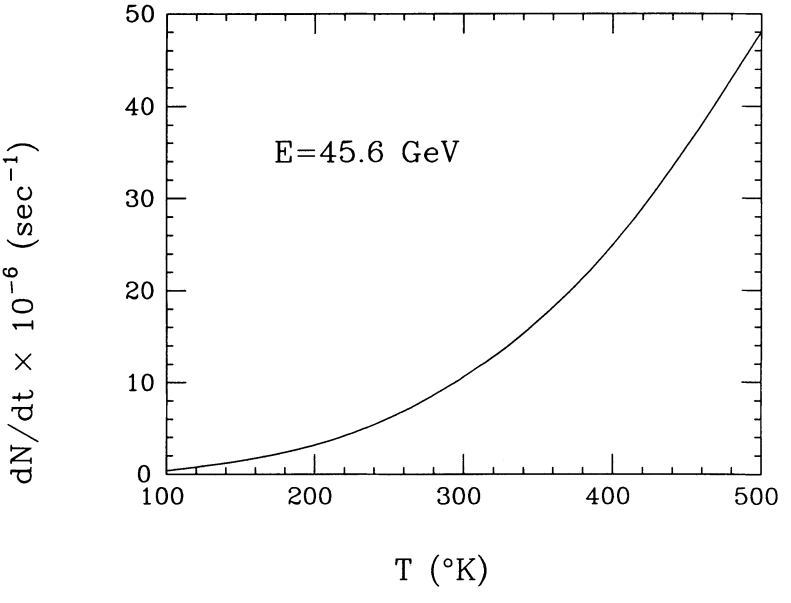

FIGURE 4: The rate $\frac{dN}{dt}$ of scattered thermal photons vs the pipe temperature T at a fixed electron beam energy $E = 45.6$ GeV.

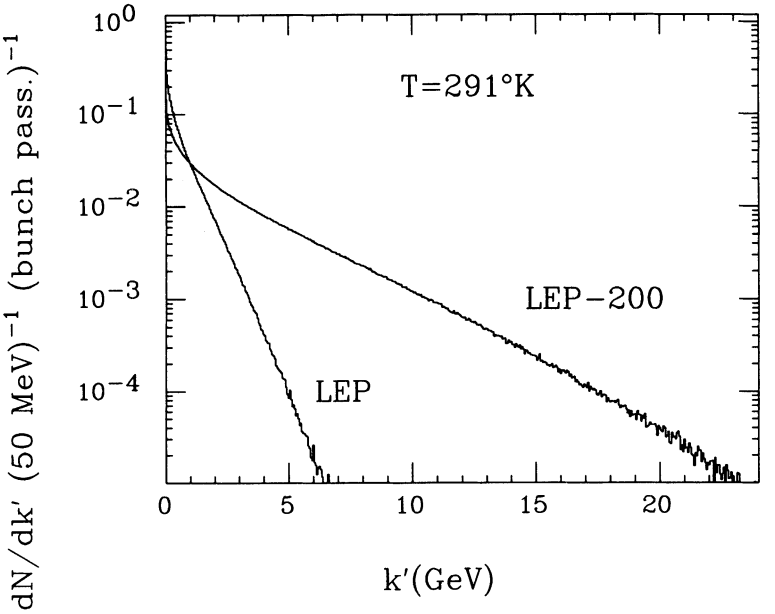

FIGURE 5: Energy spectrum of scattered thermal photons evaluated in the case of LEP and LEP-200 at a pipe temperature $T = 291°K$, for 1 mA total electron current and over a 600 mt long straight section.

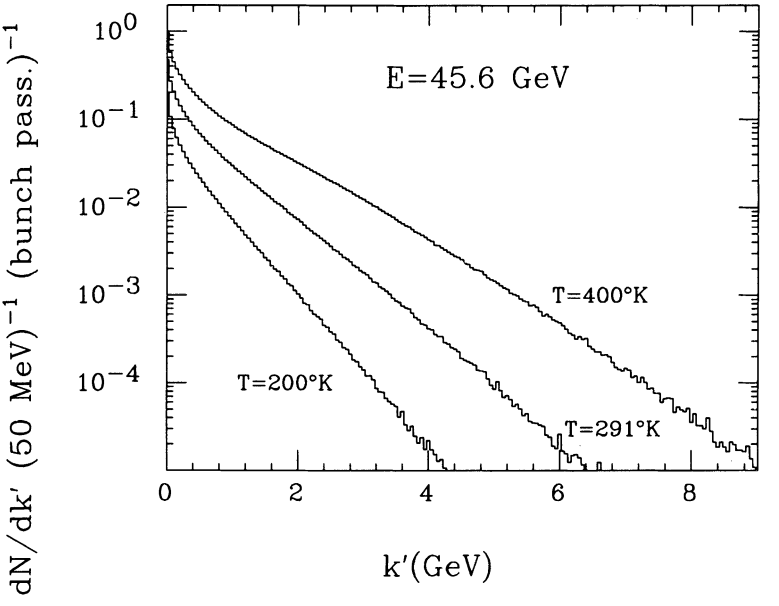

FIGURE 6: Energy spectrum of scattered thermal photons evaluated in the case of LEP at a pipe temperature $T = 200$, 291 and $400°K$, for 1 mA total electron current and over a 600 mt long straight section.

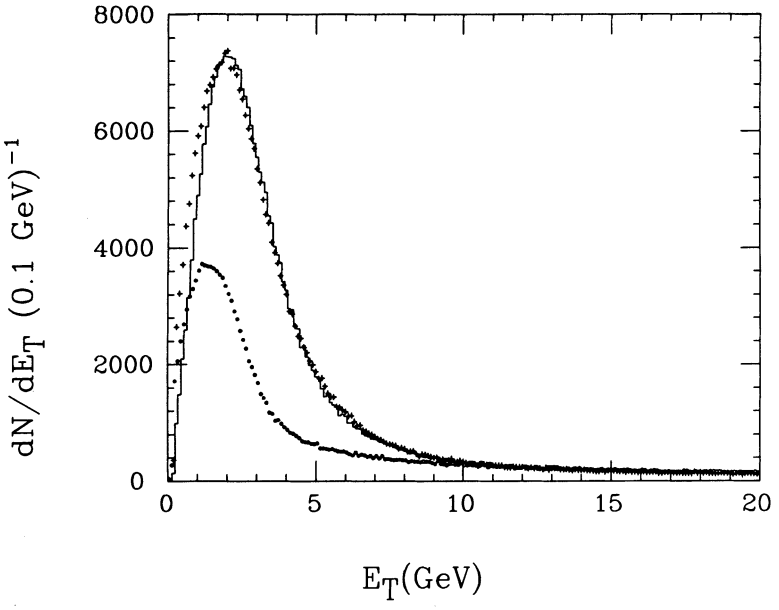

FIGURE 7: The distribution of the total energy E_T of the photons produced in the LEP straight section 1 measured at each bunch passing with the LEP-5 electromagnetic calorimeter. Experimental data up to $E_T = 20$ GeV (histogram) are compared with a Monte Carlo simulation of beam-gas bremsstrahlung (black circles) and beam-gas bremsstrahlung plus Compton scattered thermal photons (crosses).

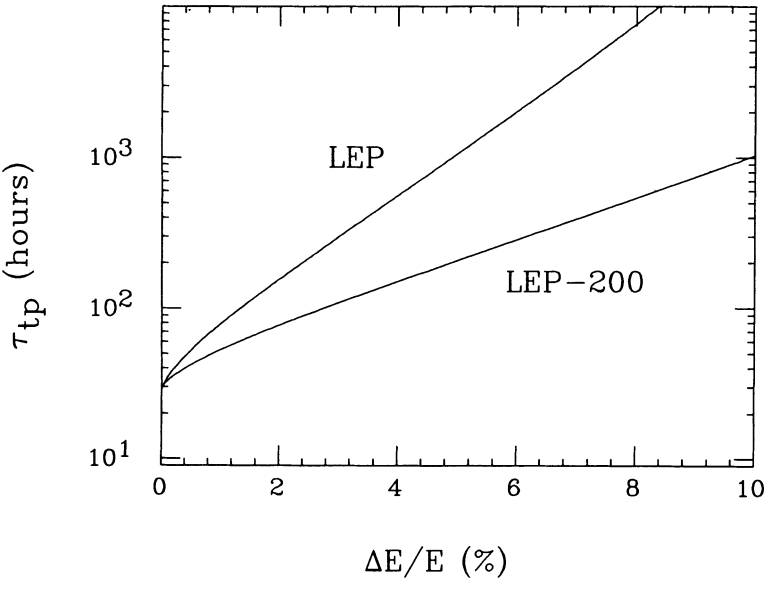

FIGURE 8: Beam lifetime due to inverse Compton scattering of thermal radiation vs the minimum fractional energy loss $\frac{\Delta E}{E}$ at which electrons leave the beam. The abscissa values are given in %.

calorimeter[1,9]. The beam energy is 46.1 GeV. Experimental data up to $E_T = 20$ GeV (histogram) are compared with a Monte Carlo simulation of beam-gas bremsstrahlung (black circles) and beam-gas bremsstrahlung plus Compton scattered thermal photons (crosses) whose spectrum has been evaluated as explained in Sect.4. The simulation also takes into account multi-photon regime and instrumental effects. The best agreement of the crosses with experimental data is obtained for a total rate value of scattered thermal photon corresponding, through eq.(13) and (11), to a pipe temperature $T \simeq 291°K$. Also the fit is consistent with a residual gas pressure $P \simeq 2.2 \times 10^{-10}$ torr. More details on experimental aspects and data analysis can be found in Ref.1,9.

In Fig.8 the beam lifetime τ_{tp} evaluated in the case of LEP and LEP-200 assuming $T = 291°K$ is plotted as a function of the fractional energy loss $\frac{\Delta E}{E}$ above which electrons leave the beam. Assuming that an electron leaves the beam at a fractional energy loss greater than $\sim 1.2\%$ in the case of LEP and $\sim 2.4\%$ in the case of LEP-200[10], the beam lifetime due to thermal photon scattering is $\tau_{tp} \simeq 90$ hours in both cases.

The mean total lifetime measured at LEP is $\tau_{tot} \simeq 14$ hours[11]. As lifetimes due to different effects must be added reciprocally, it turns out that the mean total lifetime at LEP should be $\tau_{tot} \simeq 16.6$ hours without the contribution of thermal photon scattering. So the latter is small but not negligible and sets a theoretical limit to the maximum lifetime achievable at LEP.

ACKNOWLEDGEMENTS

I would like to express my gratitude to Prof. G.Diambrini-Palazzi and to Profs G.De Zorzi and D.Zanello for suggestions and stimulating discussions on the subject. I am grateful to M.Placidi of the CERN staff for providing me with useful information about some machine parameters. I wish to thank F.Cardone for a discussion on some aspects of spectra evaluations.

REFERENCES

1. C.Bini, G.De Zorzi, G.Diambrini-Palazzi, G.Di Cosimo, A. Di Domenico, P.Gauzzi, D.Zanello , *Phys. Lett.* **B 262** (1991) 135.
2. B.Dehning, A.C.Melissinos, F.Perrone, C.Rizzo, G. von Holtey, *Phys. Lett.* **B 249** (1990) 145.
3. E. Feenberg and H.Primakoff, *Phys. Rev.* **73** (1948) 449.
4. T.M.Donahue, *Phys. Rev.* **84** (1951) 972.
5. R.J.Gould, *Am. J. Phys.* **35** (1967) 376.
6. F.C.Jones, *Phys. Rev.* **167** (1968) 1159.
7. G.R.Blumental and R.J.Gould, *Rev. Mod. Phys* **42** (1970) 237.
8. see for example L.D.Landau and E.M.Lifshits, *Teoria quantistica relativistica* (Ed. Riuniti, Rome, 1978)
9. C.Bini, G.De Zorzi, G.Diambrini-Palazzi, G.Di Cosimo A.Di Domenico, P.Gauzzi, D.Zanello, *Nucl.Instr.and Meth.* **A306** (1991) 467.
10. M.Placidi, private communication
11. E.Keil, CERN SL/91-33(AP)